Synthesis and Properties in Solution of Rodlike Polyelectrolytes

Matthias Ballauff,[1] *Jürgen Blaul,*[1] *Birgit Guilleaume,*[1] *Matthias Rehahn,**[2] *Steffen Traser,*[2] *Matthias Wittemann,*[1] *Patrick Wittmeyer*[2]

[1] Polymer Institute, University of Karlsruhe, Kaiserstrasse 12, D-76128 Karlsruhe, Germany
[2] Ernst-Berl-Institute for Chemical Engineering and Macromolecular Science, Darmstadt University of Technology, Petersenstrasse 22, D-64287 Darmstadt, Germany
E-mail: mrehahn@dki.tu-darmstadt.de

Summary: Efficient synthetic strategies are described for the preparation of rodlike polyelectrolytes based on the intrinsically rigid poly(*p*-phenylene). Uncharged precursors were first prepared via the Suzuki coupling and then characterized by different methods of polymer analysis. Finally, they were transformed into polyelectrolytes using macromolecular substitution reactions. Depending on the substitution pattern, the obtained polyelectrolytes are either soluble or insoluble in water. Using water-soluble derivatives, the Poisson-Boltzmann cell model was tested by osmotic measurements and small-angle X-ray scattering. It is shown that the cell model provides a good first approximation of the distribution of the counterions around the macroion but still underestimates their correlation. Moreover, the PPP polyelectrolytes show a very pronounced polyelectrolyte effect. Since the rodlike PPPs are very rigid in shape, this observation proves that the polyelectrolyte effect is caused by long-range intermolecular electrostatic repulsion of the dissolved macroions rather than due to conformational changes.

Keywords: cell model; counterion condensation; osmotic coefficient; polyelectrolytes; rodlike polymers

Introduction

Polyelectrolytes represent key compounds in living organisms as well as in materials and processes of our daily life. They especially show their benefits when dissolved in water. Thus, for tailor-making polyelectrolytes, profound understanding of their behavior in aqueous solutions is required. It is well-known that electrostatic forces, osmotic effects and conformational changes must be considered in detail for developing this knowledge. Consequently, much effort has been spent in analyzing this class of functional polymers, using different techniques and materials. However, a quantitative interpretation of the collected data has been impossible up to today. This is because the intramolecular and intermolecular coulomb forces — and hence all properties

 DOI: 10.1002/masy.200450701

influenced by electrostatic interactions — strongly depend on the ionic strength: at very low ionic strength, polyelectrolyte molecules repel each other over very long distances. Moreover, the electrostatic forces cause intramolecular repulsion of the chain segments. Stretching and coil expansion are consequences in the case of flexible chains. These conformational changes, however, again change the intermolecular interactions. To conclude, it is impossible to differentiate the macroscopically measured data quantitatively according to the underlying intermolecular and intramolecular electrostatic, conformational and osmotic effects without profound theoretical understanding of polyelectrolyte behavior. Conversely, however, it is impossible to develop the needed knowledge by only considering flexible polyelectrolytes. Rigid, rodlike polyelectrolytes, on the other hand, cannot change their shape significantly. Therefore they represent ideal model systems for developing the required understanding. Poly(*p*-phenylene) (PPP) seems to be the most appropriate polymer backbone here because (*i*) it is intrinsically rodlike and (*ii*) it is inert to hydrolysis and other side reactions. Hence we developed powerful synthetic routes for the preparation of PPP-based polyelectrolytes. We combined the Pd-catalyzed Suzuki reaction with the concept of solubilizing side chains, and we applied macromolecular substitution routes (route B in Scheme 1) rather than direct syntheses according to route A. This procedure was selected because in precursor strategies the polycondensation process (B1) leads to a non-ionic intermediate which can be characterized using all techniques of polymer analysis. Provided an efficient substitution reaction is available for step B2, the well-defined precursors can subsequently be converted into the desired PPP polyelectrolytes while all molecular information determined for the uncharged precursor remains valid.

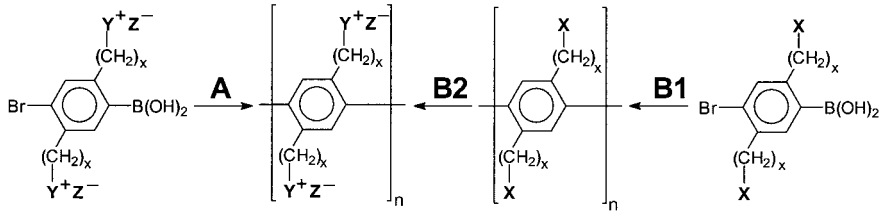

Scheme 1: Synthetic approaches to PPP-based polyelectrolytes: direct synthesis (**A**) and precursor route (**B**); X: precursor functionality, Y^+: polyelectrolyte functionality, Z^-: counterion

Synthesis of PPP Polyelectrolytes via Ether Intermediates

Aliphatic ethers were selected as precursor functionalities because they are inert under the Suzuki conditions but can be converted easily and completely into, for example, alkyl halogenides. In turn, these lateral alkyl halogenides should allow efficient introduction of ionic functionalities into the PPP in the final step.

In a first set of experiments, butoxymethylene-substituted precursor PPPs **3** were prepared.[1,2] The polycondensation of equimolar amounts of **1** and **2** leads to constitutionally homogeneous products **3** having values of $P_n \approx 60$ (Scheme 2). The lateral benzyl-alkyl ether groups were then cleaved quantitatively, leading to readily soluble bromomethylene-functionalized precursors **4** which were finally converted into carboxylated PPPs **5**, for example.

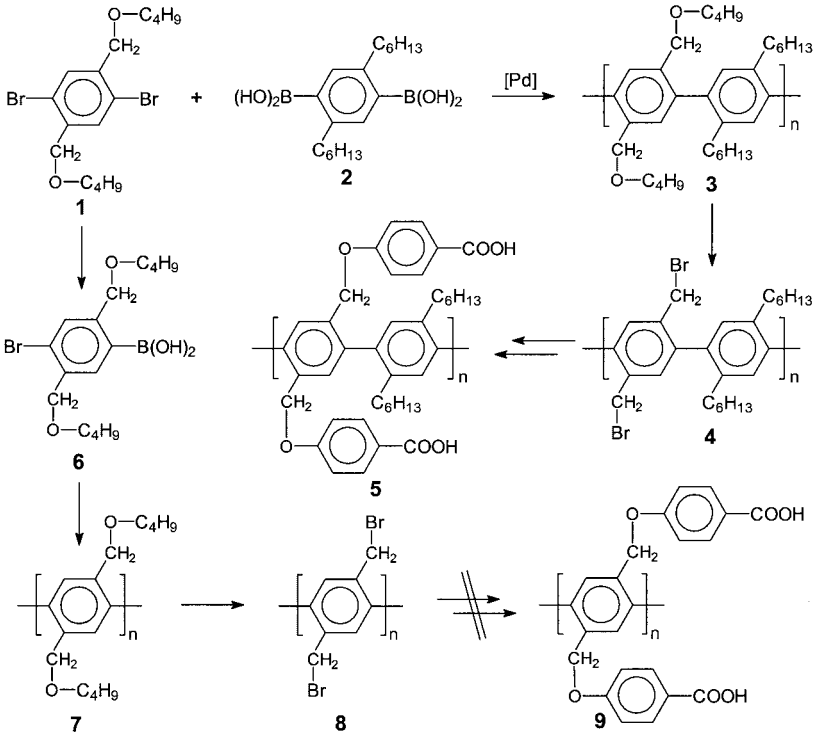

Scheme 2: Synthesis of PPP polyelectrolytes via butoxymethylene-substituted precursors

However, **5** proved to be insoluble in water or aqueous bases. We assumed that this is due to its low density of charged groups along the chains. Moreover, the apolar alkyl side chains attached to every second phenylene moiety might cause intermolecular hydrophobic interactions, leading to the observed insolubility in water. We therefore tried to prepare the corresponding homopolymer **7**. Under special conditions, we obtained the AB type monomer **6**. However, after successful polycondensation it was impossible to transfer precursor **7** into polyelectrolyte **9**: due to the lack of solubilizing side chains in the activated intermediate **8**, this material proved to be completely insoluble and thus could not be converted into a constitutionally homogeneous product **9**. This failure forced a change in the synthetic strategy. We now combined the functions of the two different lateral substituents of **3**, *i.e.* solubilizing the polymer (done by the C_6H_{13} groups) and making possible final introduction of electrolyte functionalities (done by the CH_2-O-C_4H_9 groups), in one single type of side chains.[3] This was achieved by introducing long *n*-alkyl spacers between the PPP main chain and ether functionalities. Due to the longer spacers, however, the ether oxygen moved away from the benzylic position. To nevertheless maintain the required selectivity of the ether cleavage process – which must provide 100% halogenalkyl groups to prevent crosslinking – aliphatic-aromatic ethers were applied. Hexamethylene spacers proved to solubilize the rod-like macromolecules sufficiently even after ether cleavage, leading to the activated intermediate **11**. Hence, **10** was the precursor polymer of choice.

Quite surprisingly, however, all anionic polyelectrolytes prepared from **11** such as **12** and **13** proved to be insoluble in water or aqueous bases although their charge density was twice as high as in polymers like **5**.[3] In contrast to this, cationic polyelectrolytes such as **14** - **16**, easily available via conversion of **11** with a tertiary amine, were soluble not only in polar organic solvents but even in pure water.[4,5] We believe this is due to the fact that the apolar interior of these cylinder-like polyelectrolytes is covered by a sufficiently dense and homogeneous shell of hydrophilic cationic groups which prevent intermolecular hydrophobic interactions. PPP polyelectrolytes **15** and **16** could thus be analyzed with regard to their properties in solution using osmometry, small-angle X-ray scattering and viscosimetry. Special emphasis was directed towards the so-called "counterion condensation".

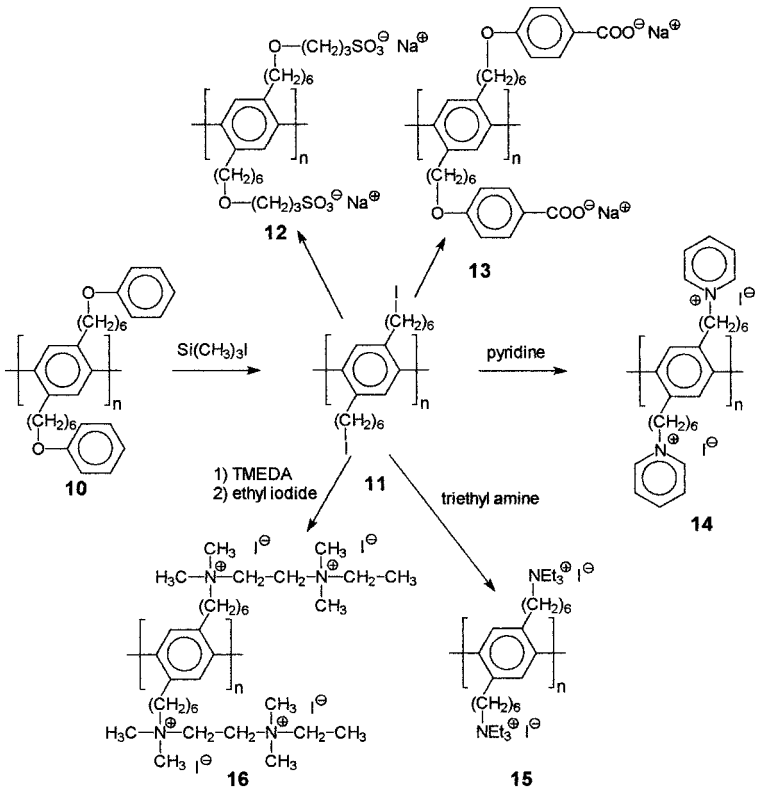

Scheme 3: Synthesis of PPP polyelectrolytes via 6-phenoxyhexyl-substituted precursor

Properties in Solution of PPPs 15 and 16

The phenomenon of counterion condensation was first described by Manning.[6,7] It appears because polyelectrolytes dissociate in polar solvents into highly charged macroions and a large number of oppositely charged small counterions. The high electric field of the macroions strongly couples to the counterions which thus partly neutralize the macroions. In turn, this strong correlation reduces the thermodynamic activity of the counterions. Only a certain fraction is osmotically active. Consequently, aqueous solutions of polyelectrolytes show a much lower osmotic pressure π than expected based on the number of counterions provided by the polyelectrolyte. This reduction in counterion activity can be expressed in terms of the osmotic

coefficient Φ. This is the quotient of the experimentally observed osmotic pressure π_{obs} and the ideal osmotic pressure π_{id} calculated for a solution of counterions interacting neither with themselves nor with the macroion:

$$\Phi := \pi_{obs} / \pi_{id}$$

A large number of experimental studies of Φ is available in the literature, demonstrating that Φ is of the order of 0.2 to 0.3 for strongly charged polyelectrolytes and univalent counterions in the dilute regime.[8] A theoretical description of the obtained data can be carried out using the so-called Poisson-Boltzmann (PB) cell model: generation of a cell model is a common way of reducing the complicated many-body problem to an effective one-particle theory, *i.e.* the case of a single polyelectrolyte chain in a cell.[8-13] The basic idea is to partition the whole solution into small sub-volumes, each containing just one single macroion together with all its counterions. Since each sub-volume is electrically neutral, the electric field will *on average* vanish on the cell surface. By virtue of this construction, different sub-volumes are electrostatically decoupled to a first approximation. One may thus hope to factorize the partition function and reduce the problem to the treatment of one sub-volume called "cell". The shape of the cell is assumed to reflect the symmetry of the polyelectrolyte itself. For a solution of rod-like polyelectrolytes with density ρ_P and rod length L this is a cylindrical cell with the radius R being fixed by the condition $\pi R^2 L \rho_P = 1$ (Figure 1).

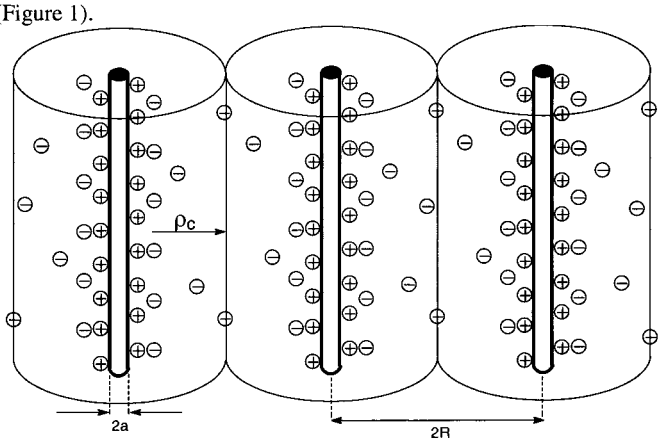

Figure 1: Polyelectrolyte rods in solution as seen by the cell model

As the theoretic treatment is again much simpler after neglecting end effects at the cylinder caps, the cylinder length is taken to be $L = \infty$ after mapping to the correct density. The ions are described as point-like, but they will electrostatically interact with the macroion as well as with each other. Their positions are thus strongly correlated. The solvent molecules are not explicitly taken into account: they are assumed to form a continuous dielectric background which is completely specified by its dielectric constant ε_r. In this simplified situation it can be proven that the osmotic pressure is defined by the counterion density at the cell boundary times the thermal energy $k_B T$.[14]

The obtained analytical description – taking into account all individual counterions – is still too involved since inter-ionic correlations complicate matters. The standard way out is to neglect these correlations in a mean-field spirit, as is done in the PB description: the ionic degrees of freedom are replaced by a cylindrical counterion density, and their interaction is approximated by the assumption that the density is locally proportional to the Boltzmann factor.[8-10,15] It can be shown that, on this mean-field level, the osmotic coefficient is defined by the ratio of boundary density and average density of the ions.[16]

For the PB treatment of the cell model, the rodlike polyelectrolyte main chain of radius a – having a contour distance per unit charge b – is coaxially enclosed in a cylinder of radius R. Electroneutrality is achieved by adding the appropriate amount of monovalent counterions, and no additional salt is present. The strength of the electrostatic interactions is conveniently expressed by the Bjerrum length

$$\lambda_B = e_0^2 / (4\pi \varepsilon_0 \varepsilon_r k_B T)$$

where e_0 is the unit charge, ε_r is the dielectric constant of the solvent, and ε_0, k_B and T have their usual meanings.[8,17] This definition suggests a dimensionless way of measuring the line charge density of the rod via the charge parameter

$$\xi = \lambda_B / b.$$

ξ counts the number of unit charges on the rod per Bjerrum length and is usually called the Manning parameter. In the PB theory the osmotic coefficient is defined[16] by the expression

$$\Phi_{PB} = \frac{1+\gamma^2}{2\xi}$$

where the dimensionless constant of integration, γ, is the solution of the transcendental equation

$$\gamma \ln \frac{R}{r_o} = \arctan \frac{1}{\gamma} + \arctan \frac{\xi - 1}{\gamma}.$$

In the limit of infinite dilution the cell radius R tends to infinity, which implies $\gamma \to 0$. For $\gamma \to 0$ and $\xi > 1$, the right-hand side of that equation tends to the constant π. Hence, the osmotic coefficient as computed by the PB theory (logarithmically) converges to the well-known Manning limiting law $\Phi_\infty = 1 / (2\xi)$. At finite densities it is always larger, however.

Unfortunately, this theoretical treatment suffers from various approximations. First, the cell model itself is a simplified representation of the polyelectrolyte solution: it neglects rod-rod interactions, is incapable of describing effects due to finite length of the rods, and reduces the solvent to a dielectric continuum. Second, the mean-field approach discards any inter-ionic correlations which can modify the average charge distribution. Furthermore, the rodlike macroions are confined in a periodic array of parallel, cylindrical Wigner-Seitz cells. On the other hand, this simplified representation greatly facilitates the solution of the PB equation. For salt-free solutions, the cell model provides an analytical expression for the distribution of the counterions around the macroion. Therefore we decided to compare the experimental results obtained by osmometry and small-angle X-ray scattering (SAXS) on the aqueous solutions of the PPP polyelectrolytes **15** and **16** with the predictions of the PB cell model.

For these investigations, it is of crucial importance that the PPP polyelectrolytes dissolve molecular-dispersly in water. Studies by SAXS (see below and Ref. [18]) and measurements of the electrical birefringence[19] demonstrate that this is the case at least in dilute solution. Moreover, the charge parameter ξ has to be known: its structural value is defined by $\xi = 3.4$ for polymer **15**, and $\xi = 6.8$ for polymer **16** (length of the repeating unit 0.43 nm, $\lambda_B = 0.73$ in water at 40 °C). The persistence length of the PPP main chain is high enough to regard these polymers as rodlike: the fully aromatic backbone of the PPPs exhibits a persistence length of approx. 20 nm.[20] The number-average contour length of PPP macroions used in the experiments is of the same order. Hence, the PPP polyelectrolytes may be treated as rod-like to a very good approximation.

Osmotic measurements

Membrane osmometry is one of the methods that allow testing of the PB cell model. We consider the system of rodlike macroions **15**, dissolved in water without added salt. In this case the PB cell model can be solved exactly to yield the osmotic coefficient for finite concentrations. As input parameters, the cell model requires the charge parameter ξ and the length L of the macroions. The other parameter necessary for the calculation of Φ is the minimum distance of contact of the macroion and the counterions, termed a. This parameter is taken from SAXS analyses shown below which gave $a = 0.7$ nm.

The osmotic coefficients were measured for two kinds of counterions, iodide and chloride, in a membrane osmometer at 40 °C. The dilute solutions were prepared in water purified by reverse osmosis and ion exchange. As a representative example, Figure 2 shows the plot of the osmotic coefficient Φ *vs.* the polymer concentration for PPP **15**.

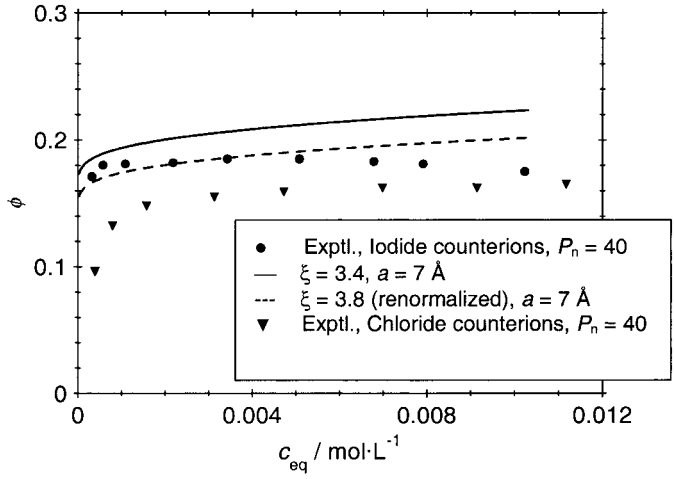

Figure 2: Osmotic coefficient Φ as a function of counterion concentration c_{eq} for PPP **15**. The solid curve is the PB prediction of the cylindrical cell model, the dashed curve is due to the correlation-corrected PB theory

Both sets of experimental data clearly indicate that the PB solution of the cell model makes a fairly good prediction of the osmotic coefficient as the dominant change in Φ, a reduction of π by a factor of 5, is correctly accounted for: the PB theory predicts Φ to vary roughly within the range 0.18 – 0.22, and the measured values accumulate around 0.18 (iodide) and 0.16 (chloride). Upon

closer look, however, the PB theory is shown to systematically overestimate the osmotic coefficient: on the enlarged scale of Figure 2 it is visible that the measured values are systematically lower than the prediction, although still higher than the Manning limit 1 / (2ξ) of infinite dilution.

The fact that the PB theory overestimates the osmotic coefficient has been observed a number of times.[8,17] Careful studies of flexible polyelectrolytes indicated that agreement between the PB cell model and experimental data could only be achieved if the charge parameter ξ was renormalized to a higher value. The motivation given for this ad-hoc modification was the assumption of a local helical or wiggly main chain. Hence, the counterions "see" more charges per unit length, *i.e.* a macroion having a higher charge parameter. However, the results obtained for stiff chain macroions **15** show that the osmotic coefficient is lower than the PB results even for systems where the local conformation of the macroions is absolutely rodlike. Therefore, this common explanation cannot be true. A part of this discrepancy between theory and experiment seems to be due to the neglect of correlations in the mean-field approach, which will lower the osmotic pressure. Moreover, it became apparent that there are specific interactions of the counterions with the macroion which can be as large as the differences from the PB solution itself. This was concluded from the fact that chloride counterions lead to a considerably smaller Φ than iodide counterions, a result which cannot be explained on the basis of the PB cell model as it stands today.[8,17] This might be interpreted in terms of hydration, but cannot be taken into account explicitly in the framework of the PB cell model. The remaining discrepancy between theory and experiment should be looked at on the level of molecular details. This includes a better description of the solvent, hydration effects, or van der Waals forces.

SAXS investigations

The goal of the following SAXS investigation was to elucidate the spatial distribution of the counterions around the macroions, and to compare the results with the prediction of the PB cell model.[18] Small-angle X-ray scattering (SAXS) has been repeatedly used to study the counterion cloud around dissolved polyelectrolytes. In many cases the contribution of the macroion to the measured SAXS intensity $I(q)$ {$q = [(4\pi/\lambda) \sin(\theta/2)]$; λ = wavelength of the used irradiation; θ = scattering angle} exceeds by far the one of the counterions. The hydrocarbon backbone of

polyelectrolytes **15** and **16**, however, exhibits a low excess electron density in water. Hence, their SAXS intensities are small, and the contribution of the counterions may become the leading term. By changing the counterions from iodide to chloride, moreover, the contrast can be changed quite drastically: while the electron density of chloride ions is nearly matched by water, iodide ions exhibit a strong contrast in aqueous solution. Hence, if iodide counterions are used, their correlation with the macroion should be easily visible. In the case of chloride counterions, on the other hand, the measured scattering intensity mainly originates from the macroions. Here, we focus our description on the iodide system.

The absolute scattering intensities $I(q)$ following from SAXS measurements may be rendered as

$$I(q) = \frac{N}{V} I_0(q) S(q)$$

where N/V is the number of dissolved polyelectrolyte molecules per volume. $S(q)$ is the structure factor which takes into account the effect of intermolecular interferences. Its influence is restricted to the region of small scattering angles. The scattering intensity $I_0(q)$ of a single rodlike polyelectrolyte molecule can be formulated as

$$I_0(q) = \int_0^1 [F(q,\alpha)]^2 d\alpha \tag{1}$$

where α is the cosine of the angle between the scattering vector q and the long axis of the molecule. The scattering amplitude of the rod with orientation α follows as

$$F(q,\alpha) = L \frac{\sin(qaL/2)}{qaL/2} \int_0^\infty \Delta\rho(r_c) J_0[qr_c(1-\alpha^2)^{1/2}] 2\pi(r_c) dr_c. \tag{2}$$

The measured scattering intensity $I_0(q)$ is thus related to the Hankel transform of the radial excess electron density $\Delta\rho(r_c)$ that can be calculated from the radial density of the macroions and the distribution of the counterions around the macroion.[18] Since the macroion has a small radius termed a, its radial electron density may be rendered in good approximation by a constant excess electron density $\Delta\rho_{rod}$. This quantity in turn can be derived from the partial specific volume of the macroion in solution.

The counterion distribution function $n(r_c)$ may be calculated from the solution of the PB equation within the frame of the cell model. Here, the polyelectrolyte is characterized by the charge parameter ξ. In order to obtain $n(r_c)$, the solution of uniform cylindrical polyelectrolytes of length

L is treated as a system of N parallel rods (see Figure 1). The cell radius R follows from the number concentration N/V of the rods as $(N/V)\ \pi\ R^2\ L = 1$. The distribution function $n(r_c)$ is defined by[21]

$$\frac{n(r_c)}{n(R_0)} = \left\{ \frac{2|\beta|}{\kappa(r_c)\cos[\beta \ln(r_c / R_M)]} \right\}^2 .$$

From the known parameters ξ, a and R, the first integration constant can be obtained through

$$\arctan\left(\frac{\xi - 1}{\beta}\right) + \arctan\left(\frac{1}{\beta}\right) - \beta \ln\left(\frac{R_0}{a}\right) = 0 .$$

The second integration constant R_M may be regarded as the radial distance within which the counterions are condensed.[21] It follows that

$$R_M = a \exp\left[\frac{1}{\beta}\arctan\left(\frac{\xi - 1}{\beta}\right)\right].$$

The screening constant κ and the number $n(R)$ of counterions at the cell boundary are related through $\kappa = 8\ \pi\ \lambda_B\ n(R) = 4(1 + \beta^2)\ /\ R^2$. With $n(r_c)$ being known – $n(r_c)$ is the excess electron density within the cell, *i.e.* for $a \le r_c \le R$ – integration of equation (2) can be performed. The number of excess electrons per counterion $\Delta\rho_{ci}$ can be calculated to a good approximation by use of their crystallographic radii. $\Delta\rho(r_c)$ follows as $= \Delta\rho_{rod}$ for $0 \le r_c \le a$, as $= n(r_c)\cdot\Delta\rho_{ci}$ for $a < r_c \le R$, and as $= 0$ for $r_c > R$. Insertion of these data in equation (2) followed by numerical integration of equations (2) and (1) then leads to the scattering intensity $I_o(q)$. The total scattering intensity of a system of non-interacting rods follows from the equation

$$I(q) = \frac{N}{V} I_0(q) S(q)$$

with $S(q) = 1$.

Figure 3 displays the absolute SAXS scattering intensities of PPP **15**.[18] In all cases, salt-free aqueous solutions with polymer concentrations c_P ranging from 3.52 up to 19.95 g·L^{-1} have been measured at 25 °C. The SAXS measurements are performed using a Kratky Kompakt camera. The scattering curves are normalized with regard to the polymer concentration (volume fraction of polymer Φ). The scattering intensities as a function of q obtained for all these solutions may be roughly divided into three regions. In the intermediate q-range, all curves decrease roughly as q^{-1}, whereas in the region of smallest values ($q < 0.4$ nm^{-1}) there is a strong rise of the measured

scattering intensity $I(q)$. At highest q-values ($q > 2.8$ nm^{-1}), on the other hand, all curves deviate from the q^{-1} dependence and decrease more drastically.

For a fit according to the PB theory, most of the required parameters are fixed experimentally, including the charge parameter $\xi = 3.4$. The only adjustable parameter is the minimum distance to which the counterions may approach the macroion. In principle, this distance is the sum of the radii of counterion and macroion. In the cell model, however, the counterions are treated as point-like objects. Therefore, this minimum distance is defined just by the radius a of the macroion. In the following fit procedure, a is treated as an adjustable parameter. Here, data were taken only for the q-values greater than 0.49 nm^{-1}: trial calculations have shown that for $q > 0.49$ nm^{-1} the influence of mutual interactions of the polyelectrolytes may be safely dismissed.[18]

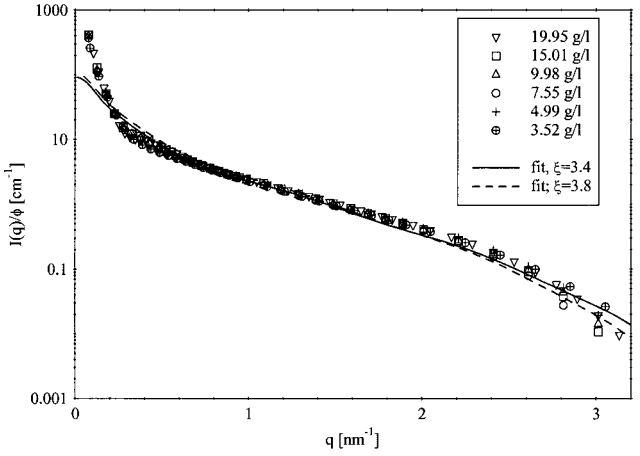

Figure 3: Comparison of measured and calculated SAXS scattering intensities for PPP **15**. The symbols give the experimental normalized scattering intensities of the aqueous solutions, the lines the optimal fits according to the PB cell model

Under these conditions, excellent agreement between theory and experiment can be achieved. Moreover, from the resulting fit, the radius a of the macroion follows as 0.7 nm. This value is considerably smaller than the value which would follow from the density of **15** in solution ($a \approx$ 1 nm). However, no meaningful description of the presented data is possible if $a = 1$ nm is assumed. This finding shows that the correlation of the counterion to the macroion is significantly

stronger than predicted by the cell model: a smaller value of a obtained from the PB cell model calculations indicates a much higher concentration of the counterions directly at the surface of the macroion than anticipated from structural data of polyelectrolyte **15**. This is in accordance with the above measurements of the osmotic coefficient of **15** in aqueous solution, and here again, this underestimation of the macroion-counterion correlation might be taken into account by increasing the charge parameter to $\xi = 3.8$.

In the preceding discussion of the experimental data we assumed that the effect of mutual interactions between the macroions is restricted to the region of smallest scattering angles, *i.e.* $S(q) = 1$ was assumed in the region from where data were used for the fit according to the cell model. However, the effect of interaction seen in the experimental scattering curves at lowest q-values should be considered as well since it is evident that there is a strong deviation between theory and experiment for $q < 0.49$ nm^{-1} in Figure 3 which points to a long-range correlation of the macroions in solution, and indicates a weak attractive interaction between the rods. This effect is seen even better in the respective scattering curves of the fourfold charged PPP polyelectrolyte **16**:[22] Figure 4 shows an enlarged view of the data in the small-angle region of PPP **16**.

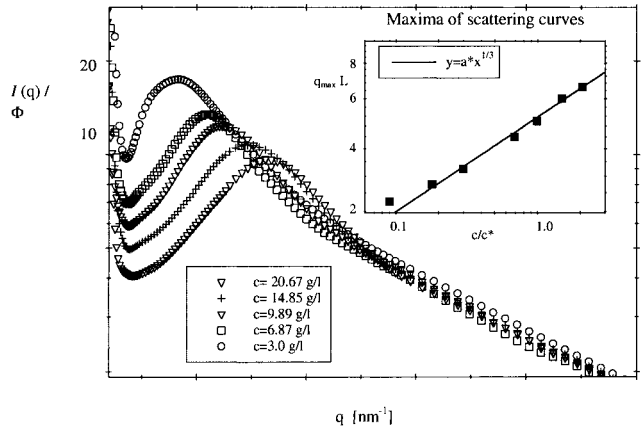

Figure 4: SAXS intensities measured for PPP polyelectrolyte **16** at small scattering angles. The inset displays the position of the maximum as a function of the concentration

A distinct maximum is evident similar to the "polyelectrolyte peak" found in salt-free solutions of flexible polyelectrolytes and of rod-like colloidal polyelectrolytes. Solutions of tobacco mosaic viruses, for example, show the position of the maximum q to depend sensitively on the concentration:[23] having defined the overlap concentration c^* of the rods through $c^* = L^{-3}$, q_{max} was found to be proportional to $(c/c^*)^{1/3}$ for concentrations smaller than c^*. For larger concentrations, the exponent ½ was found. This was taken as evidence of the onset of partial aligning of the rods due to their increased mutual interaction. It is obvious from Figure 4 that the same phenomenon also occurs in salt-free solutions of the stiff-chain polyelectrolytes **16**: the maximum scales with $c^{1/3}$ in the dilute regime (see inset in Fig. 4) whereas an exponent of ½ is found for higher concentrations. This suggests that there is some correlation in the orientation of the long axes of the polyelectrolyte molecules if the concentration exceeds c*.

Finally, at very small scattering angles ($q < 0.1$ nm^{-1}), there is a marked upturn of the scattering intensities. This could be shown to be a direct consequence of the respective upturn of $S(q)$. This may be assigned to weak attractive forces and thus correlation over the very long distances even in highly dilute systems. Hence, there is obviously some long-range interaction between the macromolecules even at very high dilutions.

Viscosity investigations

SAXS studies indicated some long-range interactions between the macromolecules even at very high dilutions. These interactions should be detectable in viscosity studies as well. Thus, viscosity measurements were carried out on salt-free and salt-containing ($NEt_4^+I^-$) aqueous solutions of PPP polyelectrolyte **15** using a capillary viscosimeter. The first question to be answered was whether or not the so-called "polyelectrolyte effect" will be observed in the Huggins plot. This effect is a matter of very controversial discussion in the literature.[24-28] There are papers which ascribe the whole effect to conformational changes, *i.e.* coil expansion as a consequence of increasing intramolecular coulomb repulsion at decreasing ionic strength. Several equations have been proposed to model the observed increase of η_{sp}/c_P at decreasing c_P such as those of Fuoss and Strauss.[29-31] However, the physical background of these equations is highly questionable because they do not describe the decrease of η_{sp}/c_P at very low c_P. Therefore, other concepts have been developed like that of Cohen, Priel and Rabin where the initial increase of η_{sp}/c_P at decreasing c_P

followed by a decrease of η_{sp}/c_P at very low c_P is assigned to the intermolecular coulomb forces:[32-36] it is assumed that dilution of a polyelectrolyte solution starts at a rather high ionic strength. Thus, upon the first dilution steps, the Debye screening length increases faster than the mean distance of the individual macromolecules (Figure 5). As a consequence, the intermolecular electrostatic repulsion increases first and thus the reduced specific viscosity. Upon further dilution, the ionic strength is more and more determined by self-dissociation of water and dissolved gasses. Consequently, the screening length increases less efficiently now compared to the mean distance of the macromolecules. Consequently, the electrostatic interaction of the macroions decreases as well as the reduced intrinsic viscosity.

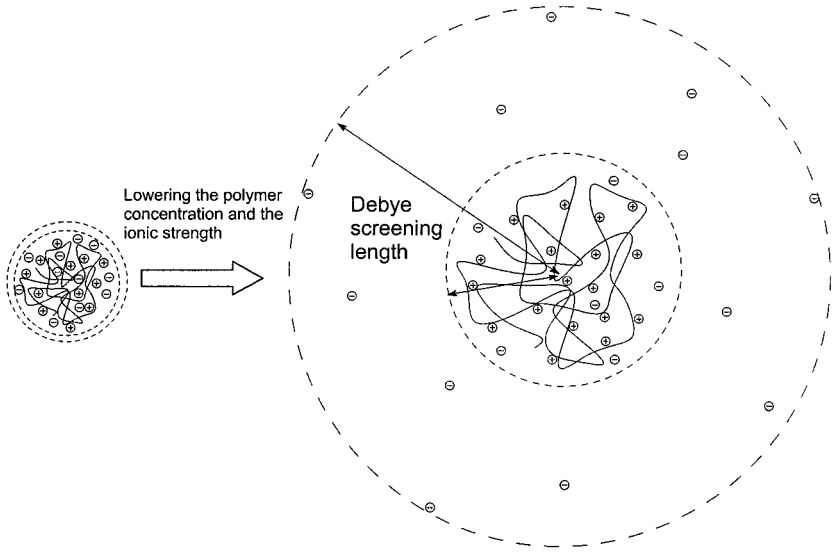

Figure 5: Schematic picture of the development of the macroion's chain conformation (inner circle) and of the Debye screening length (outer circle) of flexible polyelectrolytes in salt-free aqueous solution upon dilution

In this latter theory the unusual behavior of the reduced specific viscosity is described as a consequence of electrostatics while in the former it follows from the chain's hydrodynamic volume. Therefore, it was important to show how the intrinsically rodlike macroions such as **15** behave. In order to visualize the results, the reduced intrinsic viscosities of PPP **15** obtained in aqueous solutions[37] were plotted *vs.* the polymer concentration (Figure 6). For the salt-free case,

there is evidently a pronounced maximum of η_{sp}/c_P at $c_P \approx 5\times10^{-6}$ g·mL^{-1} while for increasing salt concentrations, this maximum becomes weaker and shifts towards higher polyelectrolyte concentrations. Finally, at salt concentrations as high as $c_s > 1\times10^{-3}$ g·mL^{-1} (not shown), the polyelectrolyte effect disappears completely, and a straight line results in the Huggins plot. Its extrapolation to $c_s = 0$ g·mL^{-1} gives an intrinsic viscosity of $[\eta] \approx 20$ mL·g^{-1}. This value is in excellent agreement with the intrinsic viscosity determined for the respective precursor PPP used for its preparation. Thus, at increasing salt concentrations, the viscosity behavior of PPP polyelectrolytes is in qualitative agreement with the behavior of flexible polyelectrolytes and naturally occurring rod-like polyelectrolytes such as DNA. However, there is a tremendous disagreement in the quantitative values, in particular at low salt concentrations.

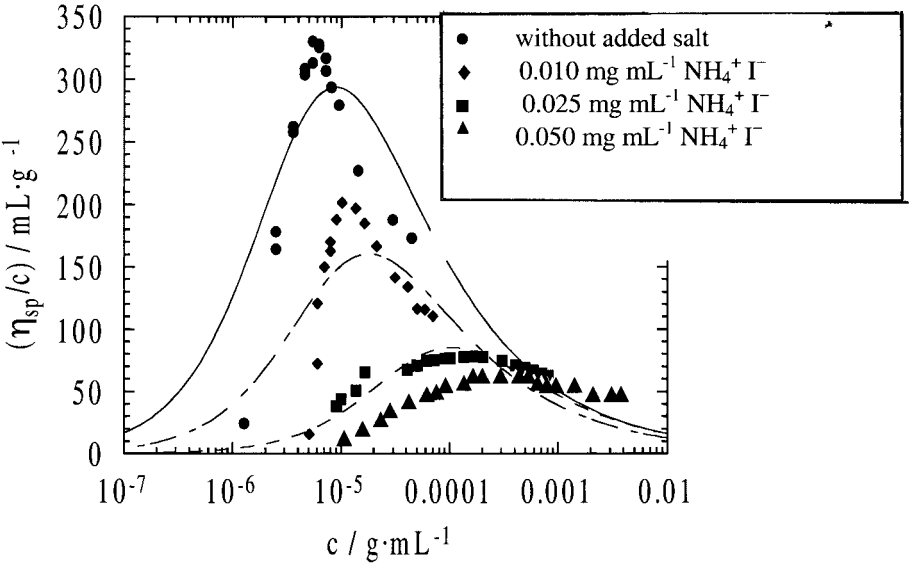

Figure 6: Plot of the reduced specific viscosities, η_{sp}/c_P, *vs.* the concentration, c_P, of PPP polyelectrolyte **15**. The lines are the best fits of the experimental data according to the Cohen-Priel-Rabbin description and shown to make obvious the drastic deviation in particular for low ionic strengths

Also, it should be emphasized that it is obviously a general feature of rodlike PPP polyelectrolytes that their maxima in the Huggins plot appear at values of c_P approx. one order of magnitude smaller than those of flexible polyelectrolytes under the respective conditions. Beyond

this, the maximum in the Huggins plot is much more pronounced and clearly narrower for PPP polyelectrolytes than for coiled macroions. The development of a detailed description of the viscosity behavior of PPP polyelectrolytes is a topic of future research. Nevertheless, it is currently clear that the so-called polyelectrolyte effect observed for flexible polyelectrolytes is certainly not the consequence of coil expansion but of long-range intermolecular electrostatic interactions.

Synthesis of PPP Polyelectrolytes via Amino Intermediates

All investigations carried out so far were performed using PPP polyelectrolytes having charge parameters ξ much larger than unity. Therefore counterion condensation was the predominant phenomenon in osmotic and scattering experiments. In order to develop a full understanding of polyelectrolytes, however, PPP polyelectrolytes with low charge parameters are required as well, *i.e.* having ξ equal to or even smaller than unity. Consequently, we prepared such PPP polyelectrolytes as well. For this purpose, the synthetic strategy shown in Scheme 4 was applied first.

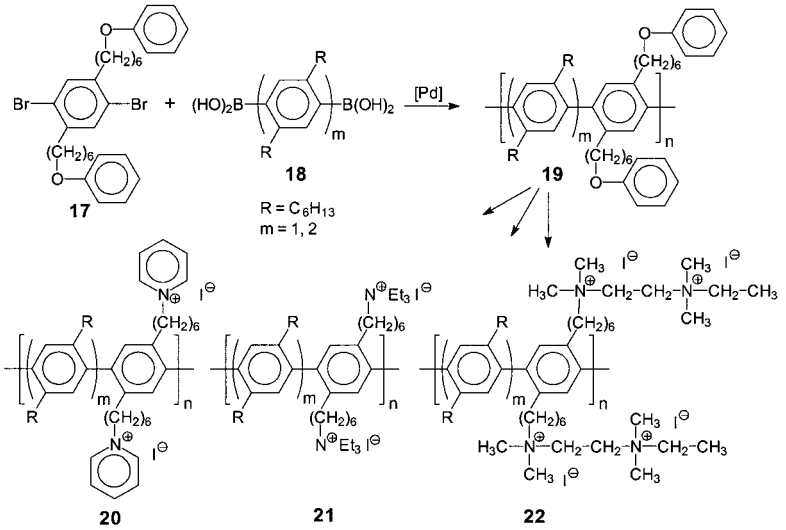

Scheme 4: First syntheses of PPP polyelectrolytes having a lower charge parameter ξ

Unfortunately, polyelectrolytes such as **20** – **22**, containing some phenylene moieties without charged side groups, proved to be insoluble in water. Insolubility in water, or dissolution only as well-defined aggregates, is also reported for similar PPP polyelectrolytes.[38-43] It seems that PPP polyelectrolytes in general need a very dense and homogeneous hydrophilic outer shell for molecular-disperse solubility in water. This shell must completely cover the cylinder-like polyions and thus suppress the hydrophobic interactions of the macromolecule's interior: if density and homogeneity of the hydrophilic shell are insufficient, intramolecular side-chain segregation occurs, leading to hydrophilic and hydrophobic areas on the macromolecule's outer shell. Experimental experience allows the conclusion that side-chain segregation and thus aggregation or precipitation of the polymers *via* hydrophobic interactions occur (*a*) when the apolar side chains are longer than the spacer groups between the polymer main chain and ionic side groups, (*b*) when the charged groups are only attached to one side of the phenylene moieties, or (*c*) in the case of polyelectrolytes such as **20** – **22** where only every second phenylene moiety bears charged side groups (Figure 7).

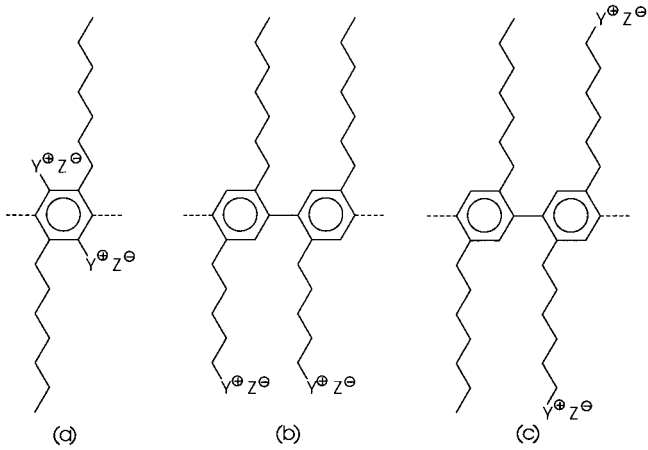

Figure 7: General motifs leading to intermolecular hydrophobic interactions of rodlike PPP polyelectrolytes and thus insolubility in water

Water-soluble PPP polyelectrolytes with charge parameter $\xi \leq 1$ therefore need non-ionic building blocks that are hydrophilic enough to prevent aggregation. Thus we developed a new synthetic strategy for PPPs which should be soluble in water even at vanishing charge density.

The key step here is the attachment of oligoethylene oxide (OEO) side chains to the PPP backbone.[44] These substituents should efficiently prevent hydrophobic interactions of the apolar PPP main chains. But the change from alkyl to OEO substituents as solubilizing side chains had some far-reaching consequences for the precursor strategy: OEO substituents do not allow the use of the above procedures where ether cleavage is a key step. Otherwise, this reaction would lead to the loss of the solubilizing side chains during precursor activation. The most convenient way to avoid ether cleavage as a macromolecular substitution step is to invert the original synthetic strategy, *i.e.* to use tertiary amines as the precursor functionalities, and to generate the polyelectrolytes via treatment of the precursor with low-molecular-weight alkyl halogenides or, alternatively, with acids (Scheme 5).[44]

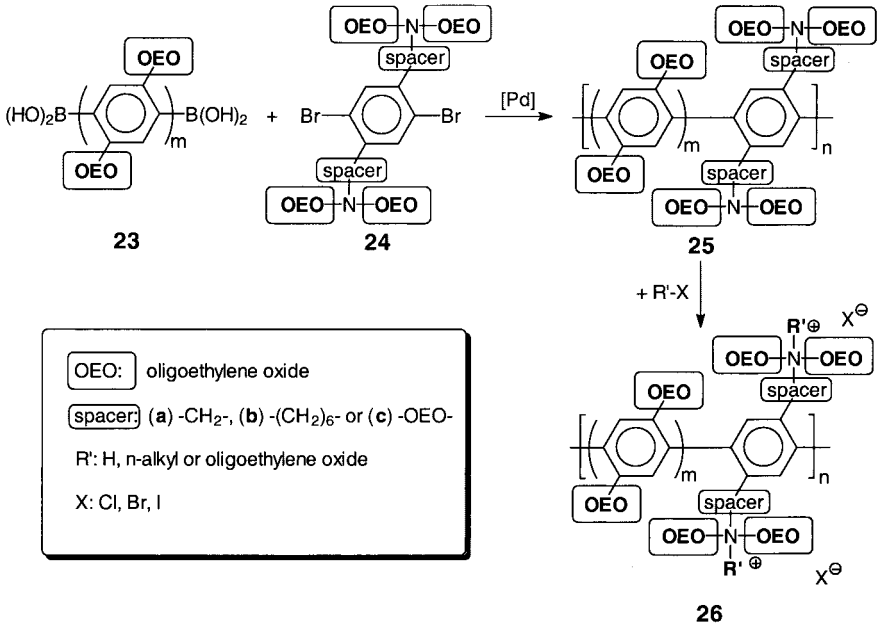

Scheme 5: Improved synthesis of PPP polyelectrolytes having a lower charge parameter ξ

Using this new strategy, we obtained the first uncharged but nevertheless readily water-soluble precursor PPPs such as **27** ($P_n \approx 30$, see Scheme 6).

Properties in Solution of Polybase 27

The new polyamine precursor PPP **27** represents a polybase because it contains amino groups in its side chains. Therefore it is of crucial importance to know the degree of protonation as a function of pH. Titration studies according to Scheme 6 show that this information is readily available using either ^{1}H NMR spectroscopy or potentiometry.

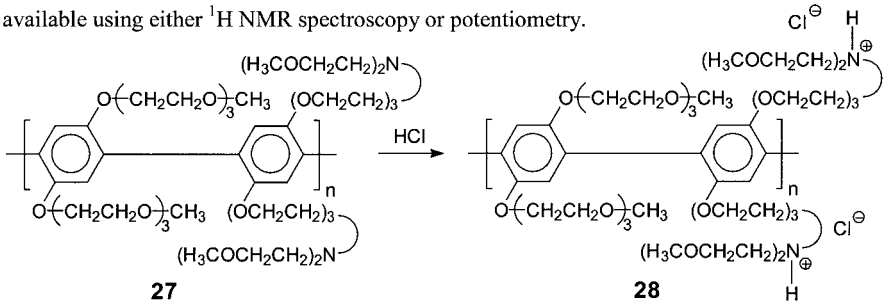

Scheme 6: Protonation of precursor PPP **27** using hydrochloric acid

It could be shown that protonation and deprotonation of PPPs **27** and **28**, respectively, take place in the range of approx. 10 > pH > 4. The determined degrees of protonation are plotted against pH for precursor PPP **27** as well as for the tris(ω-methoxyethoxyethyl)amine which was used as a low-molecular-weight reference compound (Figure 8). The circles and dots are calculated from the experimental data determined using the pH electrode (values plotted at the left y-axis). The black triangles, on the other hand, are based upon the ^{1}H NMR chemical shifts of the respective N-CH_2 protons (δ-values plotted at the right y-axis). From these data, the buffer region was determined to be between pH ≈ 6.5 and 8.5 for the monoamine, and between pH ≈ 6.0 and 8.0 for polyamine **27**. Accordingly, the precursor PPP ($pK_a \approx 7.0$) seems to be a weaker base than the monoamine ($pK_a \approx 7.5$). Based on these results, we re-calculated the curves based on the Henderson-Hasselbalch's law of mass action for degrees of protonation between 10 % and 90 %. The results are represented in Figure 8 as the solid lines. In the case of the monoamine, the data determined using the pH electrode agree very well with the expected behavior of a monobasic amine having a pK_a of 7.5. For the polymeric amine, on the other hand, there is obviously a slight deviation: the slope of the calculated curve is larger than that of the measured values. This is in agreement with previous experimental data obtained from flexible polybases. Also, it is in agreement with a model developed by Borkovec which allows the calculation of p*K* values of

polybases on the basis of Ising models. Here, microscopic p*K* values are assumed for the individual acid-base groups of the molecule which depend on the (de)protonation state of their neighboring functional groups.[45,46]

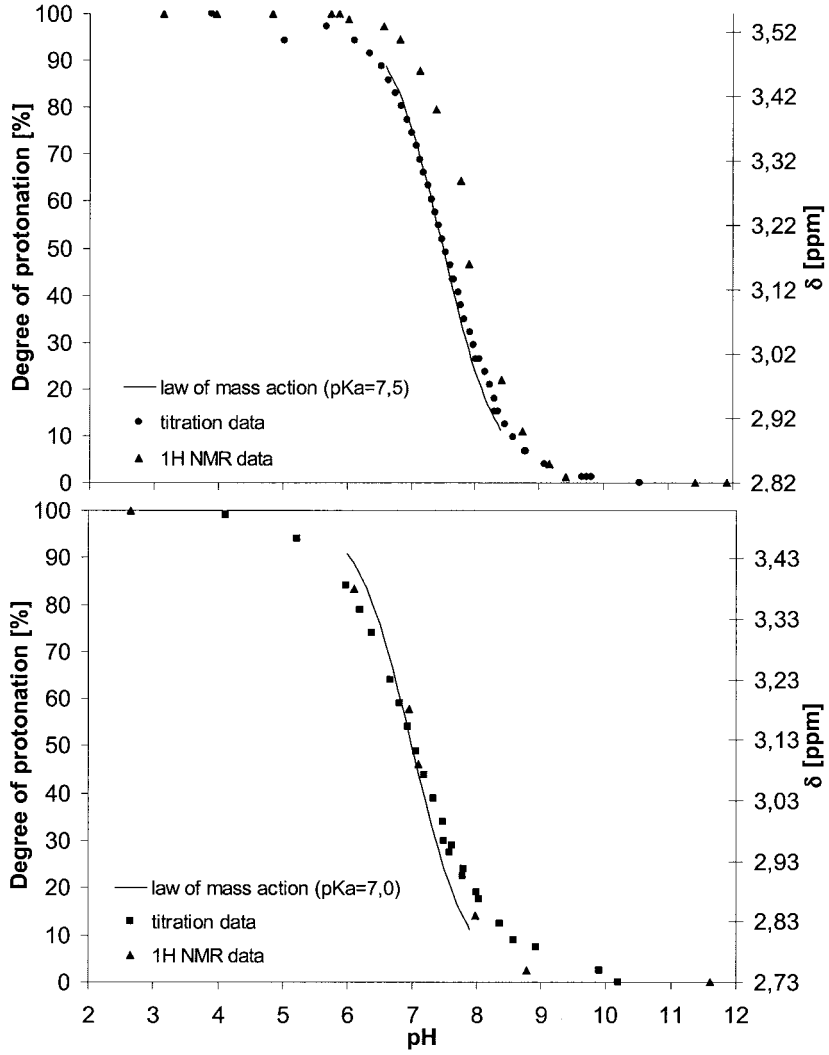

Figure 8: Degrees of protonation and ^{1}H NMR chemical shifts of the monoamine (top plot) and of precursor PPP **27** (bottom plot) as a function of pH

Conclusion

Efficient synthetic routes have been described for the preparation of rodlike PPP polyelectrolytes. Some of the obtained polymers dissolve in a molecular-disperse fashion even in pure water. For highly charged systems, the osmotic coefficient Φ proved to be a critical test for the PB cell model of rodlike polyelectrolytes. The measured data of Φ show a small but significant discrepancy compared to the PB theory. Similar conclusions were drawn from SAXS studies. These deviations may be traced back to the deficiency of the cell model which neglects ion-ion correlations as well as specific interactions between the macroions and its counterions. It became evident that the cell model nevertheless gives a semi-quantitative estimate of Φ – despite its simplicity. Moreover, for uncharged but nevertheless water-soluble PPP derivatives bearing amino groups in the side chains, it is found that the pK_a depends on the degree of protonation of the whole macromolecule. More detailed investigations concerning all these important phenomena are presently under way.

[1] I. U. Rau, M. Rehahn, *Macromol. Chem.* **1993**, *194*, 2225.
[2] I. U. Rau, M. Rehahn, *Polymer* **1993**, *34*, 2889.
[3] I. U. Rau, M. Rehahn, *Acta Polymerica* **1994**, *45*, 3.
[4] G. Brodowski, A. Horvath, M. Ballauff, M. Rehahn, *Macromolecules* **1996**, *29*, 6962.
[5] M. Wittemann, M. Rehahn, *J. Chem. Soc., Chem. Commun.* **1998**, 623.
[6] G. S. Manning, *J. Chem. Phys.* **1969**, *51*, 924, 934, 3249.
[7] G. S. Manning, *Ann. Rev. Phys. Chem.* **1972**, *23*, 117.
[8] M. Deserno, C. Holm, J. Blaul, M. Ballauff, M. Rehahn, *Eur. Phys. J.* **2001**, *E 5*, 97 and given references.
[9] R. M. Fuoss, A. Katchalsky, S. Lifson, *Proc. Natl. Acad. Sci. USA* **1951**, *37*, 579.
[10] T. Alfrey, P. W. Berg, H. Morawetz, *J. Polym. Sci.* **1951**, *7*, 543.
[11] A. Katchalsky, *Pure Appl. Chem.* **1971**, *26*, 327.
[12] K. S. Schmitz, *Macroions in solution and in colloidal suspension*, VCH Publishers, New York, 1993.
[13] M. Mandel, *J. Phys. Chem.* **1992**, *96*, 3934.
[14] L. Wennerström, B. Jönsson, P. Linse, *J. Chem. Phys.* **1982**, *76*, 4665.
[15] M. Deserno, C. Holm, S. May, *Macromolecules* **2000**, *33*, 199.
[16] R. A. Marcus, *J. Chem. Phys.* **1955**, *23*, 1057.
[17] J. Blaul, M. Wittemann, M. Ballauff, M. Rehahn, *J. Phys. Chem B* **2000**, *104*, 7077 and given references.
[18] B. Guilleaume, J. Blaul, M. Wittemann, M. Rehahn, M. Ballauff, *J. Phys.: Condens. Matter* **2000**, *12*, A245 and given references.
[19] K. Lachenmeyer, W. Oppermann, manuscript in preparation.
[20] P. Galda, *Dissertation*, Karlsruhe, 1994.
[21] M. LeBret, B. Zimm, *Biopolymer* **1984**, *23*, 287.
[22] B. Guilleaume, J. Blaul, M. Ballauff, M. Wittemann, M. Rehahn, G. Goerigk, *Eur. Phys. J.* **2002**, *E 8*, 229 and given references.
[23] E. E. Maier, R. Krause, M. Deggelmann, M. M. Hagenbüchle, R. Weber, S. Fraden, *Macromolecules* **1992**, *25*, 1125.
[24] S. Förster, M. Schmidt, *Adv. Polym. Sci.* **1995**, *120*, 53.
[25] W. Oppermann, *Makromol. Chem.* **1988**, *189*, 927.
[26] G. Weill, *J. Phys. (France)* **1989**, *49*, 1049.

[27] S. Förster, M. Schmidt, M. Antonietti, *Polymer* **1990**, *31*, 781.
[28] Y. Yamanaha, H. Matsuoka, M. Hasegawa, N. Ise, *J. Am. Chem. Soc.* **1990**, *112*, 587.
[29] R.M. Fuoss, U.P. Strauss, *J. Polym. Sci.* **1948**, *3*, 246.
[30] R.M. Fuoss, U.P. Strauss, *J. Polym. Sci.* **1948**, *3*, 603.
[31] R.M. Fuoss, U.P. Strauss, *J. Polym. Sci.* **1949**, *4*, 96.
[32] J. Cohen, Z. Priel Y. Rabin, *J. Chem. Phys.* **1988**, *88*, 7111.
[33] J. Cohen, Z. Priel, *Macromolecules* **1989**, *22*, 2356.
[34] J. Cohen, Z. Priel, *Polym. Commun.* **1989**, *30*, 223.
[35] J. Cohen, Z. Priel, *J. Chem. Phys.* **1990**, *93*, 9062.
[36] W. Hess, R. Klein, *Adv. Phys.* **1983**, *32*, 173.
[37] M. Wittemann, *Dissertation*, Karlsruhe, 1999.
[38] R. Rulkens, M. Schulze, G. Wegner, *Macromol. Rapid Commun.* **1994**, *15*, 669.
[39] S. Vanhee, R. Rulkens, U. Lehmann, C. Rosenauer, M. Schulze, W. Köhler, G. Wegner, *Macromolecules* **1996**, *29*, 5136.
[40] R. Rulkens, G. Wegner, T. Thurn-Albrecht, *Langmuir* **1999**, *15*, 4022.
[41] P. Baum, W. H. Meyer, G. Wegner, *Polymer* **2000**, *41*, 965.
[42] M. Bockstaller, W. Köhler, G. Wegner, D. Vlassopoulos, G. Fytas, *Macromolecules* **2000**, *33*, 3951.
[43] M. Bockstaller, W. Köhler, G. Wegner, D. Vlassopoulos, G. Fytas, *Macromolecules* **2001**, *34*, 6359.
[44] S. Traser, P. Wittmeyer, M. Rehahn, *e-Polymers,* **2002**, no. 032.
[45] M. Borkovec, G, J. M. Koper, *J. Phys. Chem.* **1994**, *98*, 6038.
[46] G. J. M. Koper, M. Borkovec, *J. Phys. Chem. B* **2001**, *105*, 6666.